**İSTANBUL TİCARET ÜNİVERSİTESİ**
**FEN BİLİMLERİ DERGİSİ**

*Istanbul Commerce University Journal of Science*

http://dergipark.org.tr/ticaretfbd

*Research Article / Araştırma Makalesi*

# ANALYSIS OF LARGE-SCALE PATH LOSS MODEL AT 33 GHZ IN INDOOR LABORATORY ENVIRONMENT

## BİNA-İÇİ LABORATUVAR ORTAMINDA 33 GHZ'DE BÜYÜK ÖLÇEKLİ YOL KAYBI ANALİZİ

**Cihat ŞEKER[1]** **Muhammet Tahir GÜNEŞER[2]**

https://doi.org/10.55071/ticaretfbd.954475

*Corresponding Author / Sorumlu Yazar*
*cihatseker@karabuk.edu.tr*

*Received / Geliş Tarihi*
*18.08.2021*

*Accepted / Kabul Tarihi*
*12.10.2021*

## Abstract

In this study, two important large-scale path loss models, which are Close-In (CI) model with free space reference distance and Float Intercept (FI) model, were compared in indoor laboratory scenario for fifth-generation (5G) radio systems. Comparisons are conducted using a ray-tracing-based simulation environment at ten different measurement points, at 33 GHz center frequency, and distances between 1,5 to 9 m. According to the results obtained, the one-parameter CI model is simpler and more consistent than the two-parameter FI model. CI model offers better simulation accuracy, greater simplicity, and better iterability between experiments, besides better adaptation to both line-of-sight and non-line-of-sight conditions. In addition, the CI model exhibit high stability at wide frequency ranges.

**Keywords:** CI model, FI model, indoor laboratory environment, large-scale path loss model, 33 GHz.

## Öz

Bu çalışmada, beşinci nesil (5G) radyo sistemleri için bina-içi laboratuvar ortamında iki önemli geniş ölçekli yol kaybı modeli karşılaştırılmıştır. Bu modeller, yakın mesafe (YM) referans modeli ve kayan kesme (KK) modelidir. Ölçümler ışın izleme temelli bir simülasyon programı ile 10 farklı noktada, 33 GHz merkez frekansında yapılmıştır. Verici ile alıcı arasındaki mesafe 1,5 ila 9 m arasında değişmektedir. Elde edilen sonuçlar göstermektedir ki, bir parametreli YM modeli, iki parametreli KK modelinden daha basit ve daha tutarlıdır. YM modeli, verici ile alıcı arasında görüş hattı olan ve olmayan koşullara daha iyi adaptasyon sağlayabilmektedir. Ayrıca ölçümler sırasında daha iyi simülasyon doğruluğu, daha fazla basitlik ve tekrarlanabilirlik sağlamaktadır. Bunların yanı sıra YM modeli geniş frekans aralıklarında yüksek kararlılık sergileyebilmektedir.

**Anahtar Kelimeler:** Bina-içi laboratuvar ortamı, geniş ölçekli yol kaybı modeli, kayan kesme (KK) modeli, yakın mesafe (YM) modeli, 33 GHz.

[1]Karabuk University, Faculty of Engineering, Department of Electrical-Electronics Engineering, Karabuk, Türkiye. cihatseker@karabuk.edu.tr, Orcid.org/0000-0002-9680-4622.

[2]Karabuk University, Faculty of Engineering, Department of Electrical-Electronics Engineering, Karabuk, Türkiye. mtguneser@karabuk.edu.tr, Orcid.org/0000-0003-3502-2034.

## 1. INTRODUCTION

Today, the number of personal communication devices such as smartphones and tablets are increasing rapidly. However, users' demands for data access anytime, anywhere are also growing. This situation has forced service providers to provide higher data rates and quality. New spectrums and innovative technologies are needed to meet the demand for data access. This promotes the development of innovative technology such as 5G wireless communication and a new spectrum such as the millimeter waves (mmWaves) (Agubor et al., 2019) (Haneda et al., 2016). 5G communication systems, which have just completed their development, are expected to offer revolutionary technologies while using new spectrums and unique architectural concepts (Boccardi et al., 2014) (Dahlman et al., 2021). Thus engineers who want to assist in the design of 5G communication systems need to develop channel models and new standards (Güneser & Seker, 2019). Channel characterization in the mmWave band has been performed by researchers before. Violette et al. conducted measurements in downtown Denver, wideband non-line-of-sight (NLoS) channels at 9,6, 28,8 and 57,6 GHz (Bechta et al., 2019) (Violette et al., 1988). The measurement data presented in these studies are insufficient. Channel modeling and propagation measurements were studied in the 60 GHz band outdoors in various city streets (Dupleich et al., 2019) (Løvnes et al., 1994). Stochastic channel modeling was performed site-specific (Dupleich et al., 2019). Therefore, the study was limited to Germany and Japan only (Dupleich et al., 2019). Samsung has actively worked on mmWave band measurement and channel modeling for 5G and beyond 5G mobile communication technologies (Hong et al., 2017). In this study, multibeam antenna technologies are studied rather than channel modeling for 5G mobile communication systems (Hong et al., 2017). Channel measurements were carried out in the E-band (81-86 GHz) in Helsinki, Finland. Aalto University performed measurements in the street canyon scenario for point-to-point communication (Kyrö et al., 2012). In this paper, geometry-based single-bounce channel model is developed for point-to-point communications in E-band (Kyrö et al., 2012). The single-bounce technique is insufficient for channel modelling. In our study, the shooting and bouncing rays technique is used. Extensive propagation measurements were conducted in the 28 GHz, 38 GHz and 73 GHz bands in outdoor (i.e., urban microcell (UMi), urban macrocell (UMa)) and indoor scenarios (Rappaport et al., 2015) (Rappaport et al., 2013). In these studies, temporal and spatial statistics were obtained by ray-tracing technique. The omnidirectional path loss models in dense urban environments in the 28 GHz and 73 GHz bands are examined (Maccartney et al., 2014). Measurements are carried out at various frequencies of the mmWave band in various parts of the world. There are many measurement campaigns that have not yet been studied or published, for example the measurement data in this paper have not been published yet.

In this paper, measurements were carried out in a ray-trace based simulation environment at the Engineering Faculty, Karabuk University. The indoor environment is preferred because the wavelength is small, and the attenuation is high in the mmWave band. The center frequency is 33 GHz, the bandwidth is 1 GHz. Two of the most used path loss models in the literature, the Close-In (CI) free space reference distance model, and the Floating Intercept (FI) model are compared (Al-samman et al., 2020) (Hemadeh et al., 2018) (Sun et al., 2018).

## 2. RAY-TRACE BASED MEASUREMENT

Wireless Insite software was used as a ray tracing-based simulation environment. Wireless Insite software is produced by REMCOM Inc. With Wireless Insite, complex indoor environments, urban environments, and rural environments can be simulated. Besides, it can predict the characteristics of the communication channel and electromagnetic propagation efficiently and accurately (Remcom, 2020).

### 2.1. Properties of Simulation Environment

Simulations were conducted with Wireless Insite 3.3.0.3 version. The waveform was selected as a sinusoid. The center frequency is 33 GHz, bandwidth is 1 GHz, and phase angle is 0˚ in the simulation environment. On the transmitter side, an omnidirectional antenna was used. The transmitter antenna has a gain of 20 dBi, Voltage Standing Wave Ratio (VSWR) value 1, E-plane half-power beamwidth of 45˚, and input power of 25 dBm. On the receiver side, a broadband directional pyramidal horn antenna was used. The receiver antenna has a gain of 18,5 dBi, VSWR value 1, and 3 dB beamwidth of 10˚ in E-plane and 11˚ in H-plane. Both the transmitting antenna and the receiving antenna are vertically polarized. In the simulation environment, Shooting-and-Bouncing-Rays (SBR) method was chosen as the ray-tracing method and the Full 3-D model was selected as the propagation model. The parameters used in the simulation environment are listed in Table I.

Table 1. Properties of The System

| Parameter | Configuration | Unit |
|---|---|---|
| Center frequency | 33 | GHz |
| Bandwidth | 1 | GHz |
| Transmitted signal | Continuous-wave | - |
| Transmitter and receiver antenna | Omnidirectional and directional pyramidal horn antenna | - |
| The output power of the transmitter antenna | 25 | dBm |
| Transmitter antenna height | 2,3 | m |
| Receiver antenna height | 1,6 | m |

### 2.2. Simulation Scenario

We performed simulation campaigns in the indoor laboratory on the 1st floor of the Engineering Faculty building, University of Karabuk. The simulation environment was a well-known indoor office, floor made of drywall, ceiling, and walls made of concrete, glass windows, wooden furniture, and doors. The dielectric and roughness properties of the materials used in the simulation environment for modeling the laboratory are listed in Table 2. The transmitter antenna was mounted 2,3 meters above the ground as in characteristic indoor hotspots, and the receiver antenna was mounted 1,6 meters as in characteristic handsets. In the laboratory, the transmitter antenna was fixed, the receiving antenna was positioned in 10 different locations for simulations of both line of sight (LoS) and NLoS. The directional horn antenna on the receiver side was rotated in 10˚ steps over the azimuth plane. Both omnidirectional antenna and pyramidal horn antenna were vertically polarized in all simulation tests. The simulation structure prepared in the Wireless Insite environment which is shown in Figure 1.

Table 2. Dielectric Parameters of Materials in The Simulation Environment

| Material | Dielectric constant | Conductivity | Roughness |
|---|---|---|---|
| Drywall | 2,8 | 0,001 | 0,2 |
| Concrete | 15 | 0,015 | 0,2 |
| Ceiling | 15 | 0,015 | 0 |
| Glass | 2,4 | 0,000 | 0 |
| Wood | 5 | 0,000 | 0,1 |

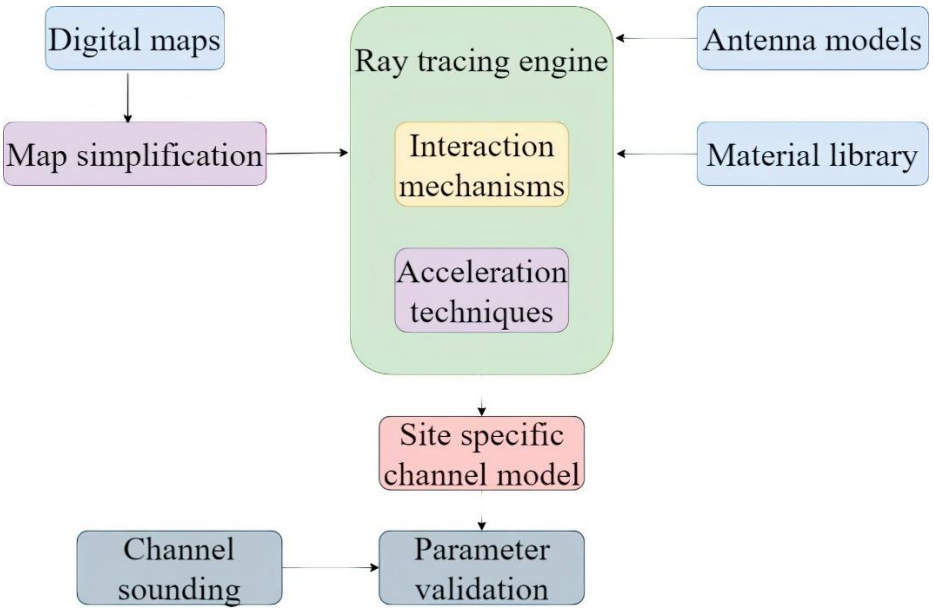


Figure 1. The Simulation Campaign System

In the case of LoS, the seperation distance between the transmitter and the receiver ranges from 1,5 m to 9 m. Ray tracing-based measurements were carried out in 1,5 m steps. Similarly, in the case of NLoS, the seperation distance between the transmitter and the receiver ranges from 9,02 m to 21,80 m and the measurements were conducted in 1,83 m steps. The indoor laboratory where the measurements were performed is 7,4 m long, 11,57 m wide and 3,3 m high. Figure 2 shows the laboratory environment where the ray-traced based study is performed. The plan of the laboratory, the transmitter position (omnidirectional antenna), and the receiver positions (red marks) are shown in Figure 3. In each of transmitter and receiver combinations, the receiver was rotated over the entire azimuth plane with 10˚ steps. For example, in the case of LoS, while the seperation distance between the transmitter and receiver was 1,5 m, the receiver was rotated 10 degrees clockwise in the azimuth plane and all channel parameters were measured. It was then rotated 20 degrees. Thus 36 different angles of arrival were obtained. Elevation plane kept constant at 0˚. The transmitter antenna kept constant at 0˚ in both azimuth and elevation planes.

Figure 2. Indoor Laboratory Environment

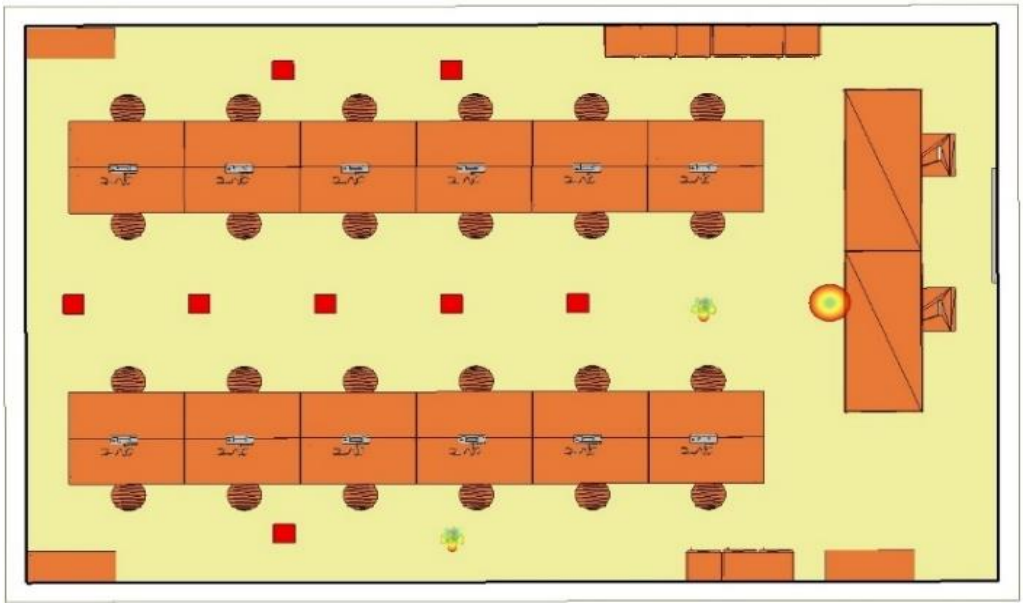

Figure 3. Top View of Laboratory Plan

## 3. LARGE-SCALE PATH LOSS MODEL ANALYSIS

Propagation models estimate the average signal power for an arbitrary separation distance between the transmitter and receiver. These models called large-scale propagation models are also useful for estimating coverage area of a transmitter. Path loss models are mathematical calculations derived to predict the transmission paths and connected losses of the signal in a given environment based on variable parameters such as distance, obstacles in the transmission path and frequency band. Path loss models are used to estimate received signal power as a function of distance. The aim of this study is to compare the performance of two different large-

scale path loss models in a indoor laboratory environment. This paper focused on CI and FI path loss models (Faruk et al., 2021).

### 3.1. Close-in Reference Distance and Floating Intercept Path Loss Models

CI and FI path loss models can predict large-scale path loss at all frequencies in a specific scenario. The formula of the CI model (Rappaport et al., 2015) is given in (1):

$$PL^{CI}[\text{dB}] = FSPL[\text{dB}] + 10n\log_{10}(d) + X_{\sigma}^{CI} \tag{1}$$

where $n$ represents the path loss exponent, $d$ denotes the 3-dimensional distance between the receiver and the transmitter, $X_{\sigma}^{CI}$ denotes a zero-mean Gaussian random variable with a standard deviation $\sigma$ and $FSPL$ represents the free space path loss in dB where the distance between the receiver and the transmitter is 1 m.

$$FSPL[\text{dB}] = 20\log_{10}\left(\frac{4\pi f}{c}\right) \tag{2}$$

where $f$ represents the carrier frequency and $c$ represents the speed of light. It is seen that the CI model uses only one parameter (path loss exponent) from the equations given above and the free space path loss value is proportional with the frequency as seen on Eq. 3 for the FI model (Svensson at al., 2007):

$$PL^{FI}[\text{dB}] = \alpha + 10\beta\log_{10}(d) + X_{\sigma}^{FI} \tag{3}$$

where $\beta$ denotes the path loss exponent, $\alpha$ denotes the offset value optimized for path loss, $d$ denotes the 3-dimensional distance between the receiver and the transmitter, $X_{\sigma}^{FI}$ denotes a zero-mean Gaussian random variable with a standard deviation $\sigma$. The coefficients $\alpha$ and $\beta$ in the FI model are generated from the measurement results.

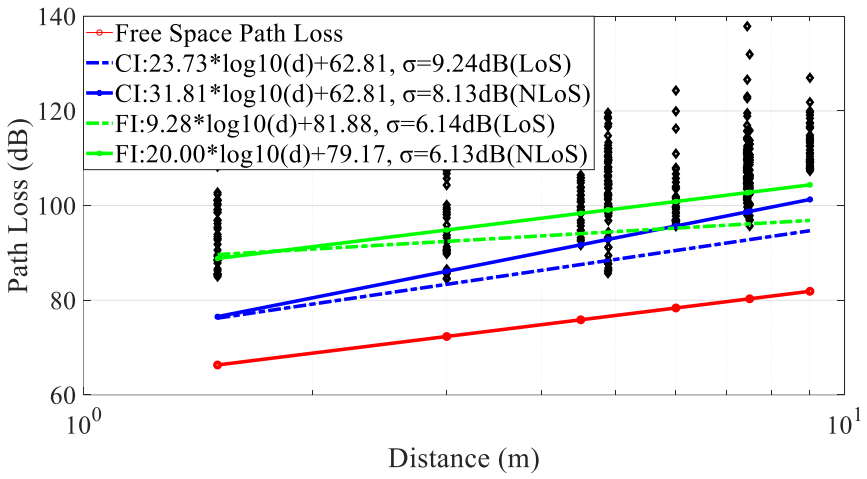


Figure 4. CI and FI Path Loss Models

The path loss models obtained using (1) and (3) are shown in Figure 4. Each column contains 36 black dots, which represent 36 path loss values acquired from 36 azimuth angles. The parameters of the two path loss models are summarized in Table 3. Compared CI model to the FI model, it was observed that the shadow fading value is higher and the path loss intercept value is smaller. The reason is that the FI model has two parameters and the parameters can be adjustable to converge to the measured value. Both the path loss exponent ($n$) parameter in the CI model $\alpha$ and $\beta$ parameters in the FI model were obtained by applying the minimum mean square error method to the path loss data obtained from the measurements.

Table 3. Parameters of Path Loss Models

| **Parameter** | | **LoS** | **NLoS** |
|---|---|---|---|
| CI | Path loss exponent | 2,373 | 3,181 |
| | Path loss intercept | 62,81 | 62,81 |
| | $\sigma$ | 9,24 | 8,13 |
| FI | Path loss exponent | 0,928 | 2,00 |
| | Path loss intercept | 81,88 | 79,17 |
| | $\sigma$ | 6,14 | 6,13 |

## 4. CONCLUSION

In this work, we compared performance of FI and CI path loss models by using a software at 33 GHz mmWave frequency in the indoor laboratory environment. The software used is based on the ray tracing method. The CI model depends on the transmitter's power and standardizes all measurements around a free space reference distance of 1 m. Thus, it provides ease of calculation for varying distances using only one parameter ($n$). The FI model has two parameters ($\alpha$ and $\beta$) that are changing quite irregularly in different frequency ranges and different scenarios. Compared to the CI model, it was observed that the FI model reduced the standard deviation by a small amount.

Regarding the results, the CI model provides a simple and one-parameter physical basis, while the FI model offers less path loss at close distances to the transmitter and greater path loss at the distances away from the transmitter, providing two parameters without a physical basis.

**Contribution of The Authors**

The contributions of the authors to the article are equal. In this study, Muhammet Tahir Güneşer contributed to the provision of ideas, criticism and computer environment. Cihat Şeker contributed to research, data collection, analysis, interpretation, literature review and writing of the article.

**Acknowledgment**

The authors would like to thank Karabuk University for their contribution in providing the simulation environment used during the study.

**Conflict of Interest**

There is no conflict of interest between the authors.

**Statement of Research and Publication Ethics**

Research and publication ethics were observed in the study.

## REFERENCES

Agubor, C.K., Akwukwuegbu, I., Olubiwe, M., Nosiri, C.O., Ehinomen, A., Olukunle, A.A., Okozi, S.O., Ezema, L. & Okeke, B.C. (2019). A comprehensive review on the feasibility and challenges of millimeter wave in emerging 5G mobile communication. *Advances in Science, Technology and Engineering Systems*, 4(3), 138-144. https://doi.org/10.25046/aj040318.

Al-samman, A.M., Azmi, M.H., Al-gumaei, Y.A., Al-hadhrami, T., Abd Rahman, T., Fazea, Y. & Al-mqdashi, A. (2020). Millimeter wave propagation measurements and characteristics for 5G system. *Applied Sciences (Switzerland)*, 10(1), 1-17. https://doi.org/10.3390/app10010335.

Al-Samman, A.M., Abd Rahman, T., Al-Hadhrami, T., Daho, A., Hindia, MHD.N., Azmi, M.H., Dimyati, K. & Alazab, M. (2019). Comparative study of indoor propagation model below and above 6 GHZ for 5G wireless networks. *Electronics (Switzerland)*, 8(1), 1-16. https://doi.org/10.3390/electronics8010044.

Bechta, K., Rybakowski, M. & Du, J. (2019, March 31 - April 5). *Efficiency of antenna array tapering in real propagation environment of millimeter wave system*. 13th European Conference on Antennas and Propagation, EuCAP, Krakow, Poland.

Boccardi, F., Heath, R., Lozano, A., Marzetta, T.L. & Popovski, P. (2014). Five disruptive technology directions for 5G. *IEEE Communications Magazine*. https://doi.org/10.1109/MCOM.2014.6736746.

Dahlman, E., Parkvall, S. & Sköld, J. (2021). What Is 5G? *In 5G NR*. Elsevier. https://doi.org/10.1016/b978-0-12-822320-8.00001-5.

Dupleich, D., Müeller, R., Landmann, M., Shinwasusin, E.A., Saito, K., Takada, J.I., Luo, J., Thomä, R. & Del Galdo, G. (2019). Multi-Band propagation and radio channel characterization in street canyon scenarios for 5G and beyond. *IEEE Access*. https://doi.org/10.1109/ACCESS.2019.2948869.

Faruk, N., Abdulrasheed, I.Y., Surajudeen-Bakinde, N.T., Adetiba, E., Oloyede, A.A., Abdulkarim, A., Sowande, O., Ifijeh, A.H. & Atayero, A.A. (2021). Large-Scale radio propagation path loss measurements and predictions in the VHF and UHF bands. *Heliyon*. 7(6), 1-15. https://doi.org/10.1016/j.heliyon.2021.e07298.

Güneşer, M. T. & Şeker, C. (2019). Compact microstrip antenna design for 5G communication in millimeter wave at 28 GHz. *Erzincan University Journal of Science and Technology*, 12 (2), 679-686. https://doi.org/10.18185/erzifbed.477293.

Haneda, K., Zhang, J., Tan, L., Liu, G., Zheng, Y., Asplund, H., Jian Li, et al. (2016, May, 15-18). 5G 3GPP-like channel models for outdoor urban microcellular and macrocellular environments. *IEEE Vehicular Technology Conference*, Nanjing, China, 1-7. https://doi.org/10.1109/VTCSpring.2016.7503971.

Hemadeh, I.A., Satyanarayana, K., El-Hajjar, M. & Hanzo, L. (2018). Millimeter-wave communications: Physical channel models, design considerations, antenna constructions, and link-budget. *IEEE Communications Surveys and Tutorials*. 20(2) 870-913. https://doi.org/10.1109/COMST.2017.2783541.

Hong, W., Jiang, Z.H., Yu, C.. Zhou, J., Chen, P., Yu, Z., Zhang, H., et al. (2017). Multibeam antenna technologies for 5G wireless communications. *IEEE Transactions on Antennas and Propagation*, 65, 6231-6249. https://doi.org/10.1109/TAP.2017.2712819.

Kyrö, M., Kolmonen, V.M. & Vainikainen, P. (2012). Experimental propagation channel characterization of Mm-wave radio links in urban scenarios. *IEEE Antennas and Wireless Propagation Letters*, 11, 865-868. https://doi.org/10.1109/LAWP.2012.2210532.

Løvnes, G., Reis, J. J. & Raekken, R. H. (1994). Channel sounding measurements at 59 GHz in city streets. *IEEE International Symposium on Personal, Indoor and Mobile Radio Communications, PIMRC*. https://doi.org/10.1109/WNCMF.1994.529139.

Maccartney, G.R., Samimi, M.K. & Rappaport, T.S. (2014). Omnidirectional path loss models in New York City at 28 GHz and 73 GHz. In *IEEE International Symposium on Personal, Indoor and Mobile Radio Communications, PIMRC*, 227-231. https://doi.org/10.1109/PIMRC.2014.7136165.

Rappaport, T.S., Gutierrez, F., Ben-Dor, E., Murdock, J.N., Qiao, Y. & Tamir, J.I. (2013). Broadband millimeter-wave propagation measurements and models using adaptive-beam antennas for outdoor urban cellular communications." *IEEE Transactions on Antennas and Propagation*, 61(4), 1850-1859. https://doi.org/10.1109/TAP.2012.2235056.

Rappaport, T.S., MacCartney, G.R., Samimi, M.K. & Sun, S. (2015). Wideband millimeter-wave propagation measurements and channel models for future wireless communication system design. *IEEE Transactions on Communications*. 63(9), 3029–3056. https://doi.org/10.1109/TCOMM.2015.2434384.

Remcom. (2020). *Wireless InSite reference manual*. *State College, PA 16801*.

Sun, S., Rappaport, T.S., Shafi, M., Tang, P., Zhang, J. & Smith, P.J. (2018). Propagation models and performance evaluation for 5G millimeter-wave bands. *IEEE Transactions on Vehicular Technology*, 67(9), 8422-8439. https://doi.org/10.1109/TVT.2018.2848208.

Svensson, T., Werner, M., Legouable, R., Frank, T. & Costa, E. (2007). "D1.1.2 WINNER II channel models: Part I channel models." *Projects. Celtic-Initiative.Org*.

Violette, E.J., Espeland, R.H., Debolt, R.O. Schwering, F. (1988). Millimeter-wave propagation at street level in an urban environment. *IEEE Transactions on Geoscience and Remote Sensing*, 26(3), 368-380. https://doi.org/10.1109/36.3038.

Xing, Y., Rappaport, T.S. & Ghosh, A. (2021). Millimeter wave and sub-THz indoor radio propagation channel measurements, models, and comparisons in an office environment. *IEEE Communications Letters*, 25(10), 3151-3155. https://doi.org/10.1109/lcomm.2021.3088264.